






## LETTER

**Trace metal contents of autotrophic flagellates from contrasting open-ocean ecosystems**

Laura E. Sofen <sup>1\*</sup>, Olga A. Antipova <sup>2</sup>, Michael J. Ellwood <sup>3</sup>, Naomi E. Gilbert<sup>4</sup>, Gary R. LeCleir<sup>4</sup>, Maeve C. Lohan<sup>5</sup>, Claire Mahaffey<sup>6</sup>, Elizabeth L. Mann<sup>1a</sup>, Daniel C. Ohnemus<sup>1b</sup>, Steven W. Wilhelm <sup>4</sup>, Benjamin S. Twining <sup>1</sup>

<sup>1</sup>Bigelow Laboratory for Ocean Sciences, East Boothbay, Maine; <sup>2</sup>X-Ray Science Division, Advanced Photon Source, Argonne National Laboratory, Lemont, Illinois; <sup>3</sup>Research School of Earth Sciences, Australian National University, Canberra, Australia; <sup>4</sup>Department of Microbiology, The University of Tennessee, Knoxville, Tennessee; <sup>5</sup>Ocean and Earth Sciences, National Oceanography Centre, University of Southampton, Southampton, UK; <sup>6</sup>Department of Earth, Ocean, and Ecological Sciences, University of Liverpool, Liverpool, UK

**Scientific Significance Statement**

Phytoplankton require iron, zinc, and other trace metals to grow. These nutrients are in short supply in many open-ocean regions where small autotrophic flagellates are important members of the ecosystem. Little is known about these cells' trace metal contents, despite many studies about the trace metal concentrations in larger phytoplankton. Across four open-ocean regions with differing levels of nutrients, we found that small, non-diatom eukaryotic phytoplankton maintain relatively low Fe concentrations, even when Fe is available in excess, a strategy that may give them a competitive advantage against plankton with higher metal demands. In addition, both Fe and Zn concentrations appear to be controlled as much by macronutrient availability as by trace metal availability.

**Abstract**

Nano- and picophytoplankton are a major component of open-ocean ecosystems and one of the main plankton functional types in biogeochemical models, yet little is known about their trace metal contents. In cultures of the picoeukaryote *Ostreococcus lucimarinus*, iron limitation reduced iron quotas by 68%, a fraction of the plasticity known in diatoms. In contrast, a commonly co-occurring cyanobacterium, *Prochlorococcus*, showed variable

\*Correspondence: [lsofen@bigelow.org](mailto:lsofen@bigelow.org); [btwining@bigelow.org](mailto:btwining@bigelow.org)

<sup>a</sup>Present address: Ronin Institute for Independent Scholarship, Portland, Maine

<sup>b</sup>Present address: Skidaway Institute of Oceanography, Savannah, Georgia

**Associate editor:** Angelique White

**Author Contribution Statement:** L.E.S. and B.S.T. co-led the manuscript effort. B.S.T., D.C.O., and M.J.E. collected the samples from the Southern Ocean. M.C.L., C.M., and E.L.M. collected the samples from the Atlantic Ocean. M.C.L. and C.M. designed the incubation experiment in the Atlantic. G.R.L. and N.E.G. designed the incubation experiment in the Southern Ocean. E.L.M. designed the culture study. B.S.T., E.L.M., and D.C.O. processed data and summarized findings. N.E.G. conducted the transcriptomic analysis. O.A.A. processed the synchrotron data. L.E.S. and B.S.T. prepared the manuscript, which was revised by M.J.E., N.E.G., G.R.L., M.C.L., C.M., E.L.M., D.C.O., and S.W.W.

**Data Availability Statement:** Cellular elemental content data and metadata are available at <https://doi.org/10.5281/zenodo.5191479>. Transcriptomic data is available at [https://genome.jgi.doe.gov/portal/Iroenrcoassembly\\_FD/Iroenrcoassembly\\_FD.info.html](https://genome.jgi.doe.gov/portal/Iroenrcoassembly_FD/Iroenrcoassembly_FD.info.html), [https://genome.jgi.doe.gov/portal/Envwatcoassembly\\_FD/Envwatcoassembly\\_FD.info.html](https://genome.jgi.doe.gov/portal/Envwatcoassembly_FD/Envwatcoassembly_FD.info.html), and <https://genome.jgi.doe.gov/portal/Algbacmetcycling/Algbacmetcycling.info.html>.

Additional Supporting Information may be found in the online version of this article.

This is an open access article under the terms of the [Creative Commons Attribution](https://creativecommons.org/licenses/by/4.0/) License, which permits use, distribution and reproduction in any medium, provided the original work is properly cited.

iron contents with iron availability in culture. Synchrotron X-ray fluorescence was used to measure single-cell metal (Mn, Fe, Co, Ni, Zn) quotas of autotrophic flagellates (1.4–16.8- $\mu\text{m}$  diameter) collected from four ocean regions. Iron quotas were tightly constrained and showed little response to iron availability, similar to cultured *Ostreococcus*. Zinc quotas also did not vary with zinc availability but appeared to vary with phosphorus availability. These results suggest that macronutrient and metal availability may be equally important for controlling metal contents of small eukaryotic open-ocean phytoplankton.

Biogeochemical models are crucial for understanding ocean function and predicting responses to changing environmental conditions. A key component of ocean models is how they parameterize nutrient uptake and storage (Flynn 2010). Iron availability controls phytoplankton abundance and community composition in much of the ocean (Moore et al. 2013), but uncertainties associated with parameters describing biological Fe processes drive large variability in predictions of future production across trophic levels (Tagliabue et al. 2020).

Leading biogeochemical models represent phytoplankton communities with three functional types—diatoms, pico-/nanophytoplankton, and small diazotrophs (Moore et al. 2018; Tagliabue et al. 2020; Stock et al. 2014)—but measurements of micronutrient requirements have typically focused on diatoms and, to a lesser extent, cyanobacteria. The pico-/nanophytoplankton, many of which are flagellated and will be referred to hereafter as “flagellates,” dominate open-ocean ecosystems (Hirata et al. 2011) and may have unique biogeochemical roles. For example, *Phaeocystis* plays a key role in the global sulfur cycle by contributing disproportionately to DMS production (Wang et al. 2015). These taxa are thought to efficiently compete for scarce dissolved nutrients (Cuvelier et al. 2010), yet less is known about their metal physiology than that of diatoms and cyanobacteria.

Data available for open-ocean flagellate strains suggests that this group may be less responsive to metal gradients than diatoms or dinoflagellates. Iron quotas of cultured *Pelagomonas calceolata*, a small flagellate isolated from the North Pacific Ocean, showed limited physiological plasticity (Sunda and Huntsman 1995), while Fe quotas of diatoms in the same study varied 100-fold. Iron quotas of small flagellated autotrophs from the equatorial Indian and Pacific Oceans also showed muted (ca. twofold) responses to natural and amended dFe gradients, respectively, (Twining et al. 2011, 2019). In the subarctic Pacific, growth rates of small (< 5  $\mu\text{m}$ ) phytoplankton are less restricted by Fe limitation than those of diatoms both in silico and in the field (Zhang et al. 2021). Thus, small flagellate taxa may gain ecological advantage through effective competition for scarce nutrients rather than through physiological plasticity and nutrient storage capacity.

To address the paucity of data on the response of Fe quota to Fe limitation in smaller phytoplankton, we cultured a globally abundant picoeukaryote and a commonly co-occurring prokaryote. We then compared metal quotas of small open-ocean autotrophs to understand the extent of variation in chemical composition in natural settings. We report metal

contents of such cells from four open-ocean regions with contrasting nutrient availability. Deckboard incubation experiments provide additional insight into cell nutrient status. This work helps inform biogeochemical models by constraining the chemical composition of a dominant phytoplankton group in open-ocean regions.

## Methods

We determined the metal contents of an isolate of the picoeukaryote *Ostreococcus lucimarinus* (CCMP 3630) using ICP-MS (full details in Supporting Information S1). *Ostreococcus* were grown under trace metal clean conditions (Cohen et al. 2018) in low-Ni B1 media at 100  $\mu\text{mol photon m}^{-2} \text{ s}^{-1}$  irradiance under both Fe-replete (100 nM total Fe, 1.2 nM Fe') and Fe-limited (7.5 nM total Fe, 86 pM Fe') conditions (see Supporting Information S1 for culturing details). In addition, two strains of *Prochlorococcus*, MED4 (CCMP 2389) and MIT9312 (CCMP 2777), were cultured to compare the responsiveness of Fe quotas in this picoeukaryote competitor. The cyanobacteria were grown in the same media and Fe concentrations as *Ostreococcus* but at 60 and 200  $\mu\text{mol photon m}^{-2} \text{ s}^{-1}$  irradiance.

Phytoplankton samples were collected at or below the surface mixed layer (SML) on three cruises of opportunity that covered a range of Fe, Zn, and macronutrient availability (Fig. 1A). Samples from the Atlantic Ocean were collected aboard the *RRS James Cook* (cruise JC150) from 26 June 2017 to 12 August 2017 (details provided by Artigue et al. 2020 and Kunde et al. 2019). We sampled from 40 m at stations at the western end of an Fe-dust gradient (22°N, 54°W; Western Atlantic, high dFe, SML 22 m) and the eastern end (22°N, 31°W; Eastern Atlantic, low dFe, SML 38 m). Samples from a transect of the Indian Ocean were collected from 20 m aboard the *R/V Roger Revelle* (cruise RR1604) during the GO-SHIP IO9N cruise from 22 March 2016 to 24 April 2016, as described previously (Twining et al. 2019). The Southern Ocean Time Series site (140°E 47°S), located in sub-Antarctic waters, was sampled at the SML (15, 30, or 40 m) multiple times from 5 to 18 March 2018 aboard the *RV Investigator* (cruise IN2018\_V02). On each cruise, phytoplankton were collected for single-cell trace metal analysis using trace metal clean techniques (Twining et al. 2019; detailed methods in Supporting Information S1).

Cellular metals were analyzed following published methods (Twining et al. 2019) at the Advanced Photon Source, Argonne National Laboratory microprobe beamline 2-ID-E. Cellular elemental concentrations (Fig. S6, Sofen and Twining 2021) were

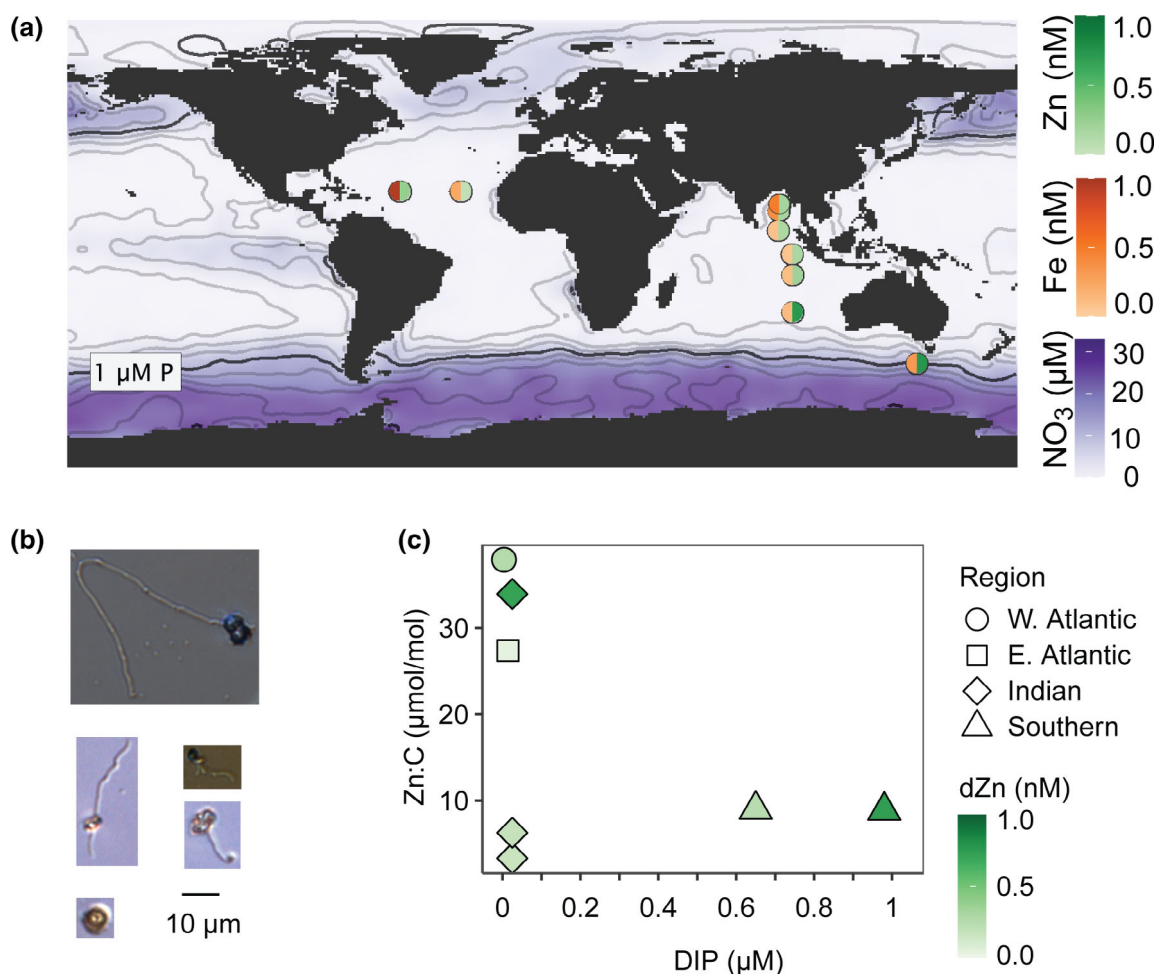


**Fig. 1.** Biogeochemical context. **(A)** Nutrient regimes. Cells were analyzed from different regions across a range of nutrient concentrations: Nitrate (background shading), phosphate ( $0.25 \mu\text{M}$  contours), dFe (left half-circle), and dZn (right half-circle). **(B)** Representative cells, light microscope images. Morphological features were compared to known traits of common nanoplankton classes. **(C)** Geometric mean cellular Zn quotas as a function of dissolved inorganic phosphorus (DIP) and Zn availability (shading). Indian Ocean DIP was below the detection limit ( $50 \text{ nM}$ ) and is plotted at  $25 \text{ nM}$ .

normalized to cellular C contents, which were calculated from cell volume using the relationship of Menden-Deuer and Lessard (2000). Light microscope images (Fig. 1B) were compared to published texts (Tomas 1997; Scott and Marchan 2005) to confirm that the analyzed cells were consistent with common nano- and picoeukaryote classes from these regions.

On each cruise, deckboard incubations were conducted to assess the physiological state of resident phytoplankton. Full details are available in Supporting Information S1 (Atlantic and Southern Oceans) and Twining et al. (2019, Indian Ocean). In the Atlantic and Indian Oceans, bottles were amended with  $\text{FeCl}_3$ ,  $\text{ZnCl}_2$ , nitrate, or a combination of these. In the Atlantic, community responses in chlorophyll *a* (Chl *a*) and alkaline phosphatase activity (APA) were measured for all incubations, and cellular metal quotas were measured from select incubations (W. Atlantic:  $2 \mu\text{M}$  nitrate and  $2 \mu\text{M}$  nitrate +  $1 \text{ nM}$  Zn; E. Atlantic: unamended control,  $0.5 \text{ nM}$  Fe, and  $0.5 \text{ nM}$  Zn). In

the Southern Ocean, bottles were amended with Fe or the Fe chelator desferrioxamine B (DFB) to adjust Fe availability (Gilbert et al. 2022). Eukaryotic transcript profiles were queried for the Fe stress markers *fld* (flavodoxin), *fea1* (Fe-assimilating protein), and *PETE* (plastocyanin), proteins produced by algae in response to cellular Fe deficiency (Roche et al. 1996; Erdner and Anderson 1999; Peers and Price 2006; Behnke and LaRoche 2020).

## Results and discussion

### Response of picoplankton Fe quotas to Fe availability in culture

Although limited data suggest that small phytoplankton may lack the high plasticity of Fe quotas seen in diatoms and large flagellates (Table S2; Sunda and Huntsman 1995), the paucity of quota data for these smaller taxa limits our understanding of how generalizable this trend is. To address this,

we investigated the Fe plasticity of a model picoeukaryote in culture. We measured Fe content of *O. lucimarinus* grown in both Fe-replete and Fe-limited media. *O. lucimarinus* is among the smallest known eukaryotic phytoplankton and was isolated from the North Pacific. It reduces its cellular Fe contents under Fe-limitation (Botebol et al. 2017). When grown under Fe-limited conditions, *O. lucimarinus* growth was reduced by 33% ( $0.59 \pm 0.01 \text{ d}^{-1}$ , mean  $\pm$  SD) relative to replete Fe ( $0.86 \pm 0.08 \text{ d}^{-1}$ ), and its Fe quota was reduced by 68%, from  $28 \pm 7$  to  $9 \pm 6 \mu\text{mol Fe mol C}^{-1}$  (Fig. 2C, Table S2). Iron quotas for the Fe-replete culture were 38% lower than reported quotas for *Emiliania huxleyi* in replete media ( $45 \mu\text{mol Fe mol C}^{-1}$ ), and substantially lower than maximum quotas in diatoms ( $68\text{--}300 \mu\text{mol Fe mol C}^{-1}$ ), while quotas for the Fe-limited culture were slightly higher than *E. huxleyi* and comparable to diatoms in limited media (3 and  $10 \mu\text{mol Fe mol C}^{-1}$ , respectively; Sunda and Huntsman 1995). This further supports that at least some small open-ocean phytoplankton taxa show reduced plasticity of Fe quotas. This may be due to differences in Fe storage capacity; for example, a related *Ostreococcus* strain (*Ostreococcus tauri*) uses the Fe storage protein ferritin for short-term Fe cycling rather than for long-term storage (Botebol et al. 2017).

*Ostreococcus* Fe quotas were compared to those of *Prochlorococcus marinus*, a cyanobacterium that is abundant in the low- and mid-latitude open ocean and a competitor to small flagellates. *Prochlorococcus* partitions into distinct ecotypes—with unique responses to Fe limitation (Rusch et al. 2010)—along environmental gradients. Under moderate irradiance ( $60 \mu\text{mol photon m}^{-2} \text{ s}^{-1}$ ), the MED4 strain of *Prochlorococcus* had similar Fe concentrations ( $32 \mu\text{mol Fe mol C}^{-1}$ ) to *Ostreococcus* grown in replete Fe and showed hardly any variation in Fe:C as a function of growth rate (Table S2, Fig. S3, detailed discussion in Supporting Information S1). In contrast, quotas of another *Prochlorococcus* strain, MIT9312, were reduced ca. twofold as growth rate was limited by Fe, from  $27$  to  $14 \mu\text{mol Fe mol C}^{-1}$ . Neither strain showed significant differences in Fe quota under high irradiance ( $200 \mu\text{mol photon m}^{-2} \text{ s}^{-1}$ ) in replete media. MED4 and another *Prochlorococcus* strain, MIT1214, have previously been found to take up additional iron after Fe repletion was achieved (Shire and Kustka 2015). This luxury uptake and the variable Fe content in one strain that we measured (MIT9312) are slightly muted compared to diatoms but much more variable than the consistently low Fe quotas that we observed in another strain (MED4) and *Ostreococcus* in culture. This highlights the surprising lack of plasticity in *Ostreococcus*, and led us to investigate natural communities of similar taxa to understand whether this response was generalizable.

### Response of Fe quotas to Fe availability in natural environments

Sampling locations spanned a range of nutrient concentrations (Fig. 1A). The Southern Ocean had high N and P, while the other three regions had low macronutrients. Dissolved Fe

varied 14-fold between regions and was low in the Southern Ocean (0.15–0.35 nM), Indian Ocean (0.07–0.49 nM), and Eastern Atlantic (0.23 nM) but high in the Western Atlantic (0.95 nM). Dissolved Zn was high in the Southern Ocean (0.24–0.74 nM), moderate in the Indian Ocean (0.15–0.21 nM at five stations; 0.72 nM at one station) and Western Atlantic (0.25 nM), and low in the Eastern Atlantic (0.04 nM).

Cellular Fe quotas of small flagellates from these four regions were strikingly consistent over the 14-fold range of dFe (Fig. 2A). Iron quotas did not vary significantly between regions (Tables 1 and S1,  $p = 0.37$ ) nor with dFe ( $p = 0.39$ ), similar to the muted responses of the model species *Ostreococcus* and *P. calceolata* in culture. This contrasts with the large ranges of quotas previously shown for cultured diatoms and larger flagellates under varying dFe (Sunda and Huntsman 1995). The narrow range of quotas we observed also contrasts with the large variability in quotas previously observed for similar flagellated cells across a dFe gradient from coast to open ocean, over which flagellate community composition likely shifted (Twining et al. 2021). Quotas measured here match the open-ocean communities from that study ( $10 \mu\text{mol Fe mol C}^{-1}$ , Fig. 2A) and from an upwelling zone of the equatorial Pacific ( $14 \mu\text{mol Fe mol C}^{-1}$ , Twining et al. 2011), despite much higher dFe at some of our stations. Measured quotas are smaller and more constrained than another study in the Atlantic: they are less than half the cellular concentrations previously measured in slightly larger autotrophic flagellates from GA03 cruise ( $35 \pm 2 \mu\text{mol Fe mol C}^{-1}$ , Twining et al. 2015). This may also be due to taxonomic differences (cells in the previous study were slightly larger) or due to seasonal changes in growth rate, as previous work occurred in the winter when growth rates were likely lower, potentially lowering metal demand but also growth dilution of Fe quotas. Flagellate quotas in the Atlantic are also lower than quotas in several co-occurring *Synechococcus* cells ( $30 \pm 4 \mu\text{mol Fe mol C}^{-1}$ ). In addition, they are lower than the maximum quota parameter in the biogeochemical model PISCES-v2 ( $\text{Fe:C}_{\text{max}} = 40 \mu\text{mol Fe mol C}^{-1}$ ) but not far from the model's optimal quota ( $7 \mu\text{mol Fe mol C}^{-1}$ , Aumont et al. 2015). While the specific taxonomic groups comprising these flagellate populations may vary between regions, the consistency shown by this common phytoplankton functional type is remarkable.

Deckboard incubations and transcriptomic measurements were used to assess the Fe status of the same open-ocean communities we analyzed for Fe contents, with the goal of assessing whether the observed low plasticity was due to physiological Fe demand or to Fe availability. We saw little evidence for Fe limitation in the phytoplankton community from the low-dFe East Atlantic: Chl *a* concentrations (Fig. S2a) did not change with Fe addition, nor did Fe quotas (Fig. 2B). In the Indian Ocean, chlorophyll concentrations did not change significantly even as Fe quotas increased fourfold upon Fe addition (Twining et al. 2019). We used transcriptomics to evaluate the physiology of Southern Ocean

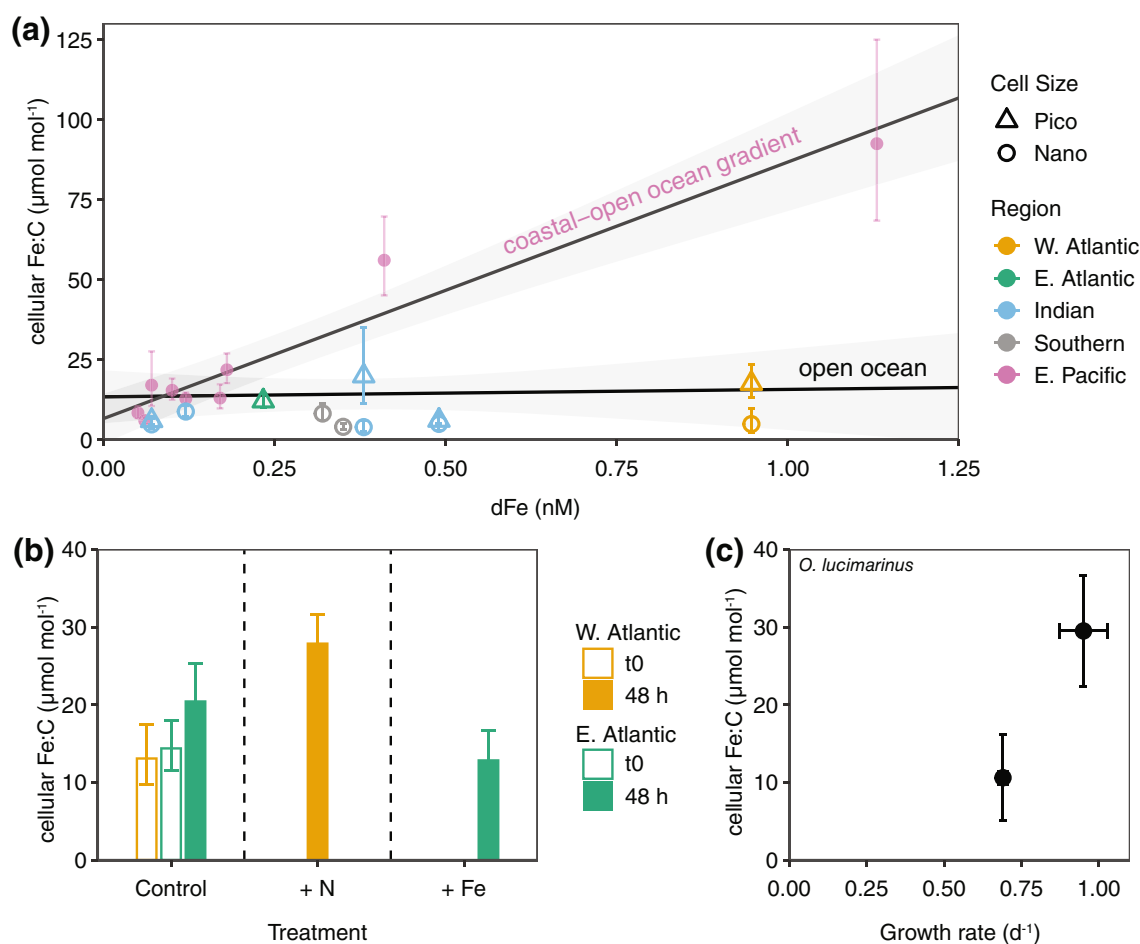


**Fig. 2.** Cellular Fe quotas across natural and artificial nutrient gradients. **(A)** Geometric mean ( $\pm$  SE) Fe quotas of small flagellates across open ocean regions of different dFe concentrations (open symbols) and along a coastal–open ocean gradient in the E. Pacific (filled symbols, 1.6–16.6  $\mu\text{m}$  cells; Twinning et al. 2021). Regressions of each data set (black lines) and 95% CI (gray shading) are shown. **(B)** Response of flagellate Fe quotas to 2  $\mu\text{M}$  nitrate and 0.5 nM Fe addition (mean  $\pm$  SD,  $n = 3$ ), E. Atlantic treatments (green) are not statistically different, W. Atlantic treatments (yellow) are different ( $p = 0.01$ ). **(C)** Cultured *O. lucimarinus* quotas in limited (7.5 nM  $\text{Fe}_T$ ) and replete (100 nM  $\text{Fe}_T$ ) culture (mean  $\pm$  SD,  $n = 3$ ;  $t(4) = 2.8$ ,  $p = 0.03$ ).

communities. The expression levels of *fld*, *fea1*, and *PETE* genes encoding common markers of cellular Fe-stress (flavodoxin, Fe-assimilating protein, and plastocyanin, respectively), were compared between in situ samples and incubations with added Fe (“high Fe”) or added DFB (“low Fe”). Expression of *PETE* by dominant phytoplankton groups did not vary with Fe availability. Meanwhile, expression of *fld* and *fea1* show that at least some groups (Haptophyta and Ochrophyta) were likely experiencing Fe-stress, indicated by similar elevated expression of *fld* and *fea1* in the low-Fe incubation and in situ surface samples (Fig. 3). However, despite this apparent Fe stress, quotas of this community approached the values associated with maximum growth in Fe-replete culture. Notably, the minimum Fe quotas we measured are not as low as the minimum quotas reported for Southern Ocean diatoms in Fe-limited culture (0.4  $\mu\text{mol Fe mol C}^{-1}$  at  $\text{Fe}^+ = 0.03$  pM, Strzepek et al. 2011). It thus appears that there

is little variability in cellular Fe concentration in potentially Fe-stressed flagellates, like the non-Fe limited flagellates from the Atlantic. These open-ocean flagellate communities may gain ecological advantage through effective competition for low nutrients rather than through physiological plasticity and nutrient storage.

#### Response of metal quotas to macronutrient availability in natural environments

While flagellate quotas showed little response to dFe, we did observe a response to macronutrients. Eukaryotes require Fe to assimilate nitrate (Schoffman et al. 2016), so Fe quotas may increase with higher nitrate assimilation. Picoeukaryotes in the Sargasso Sea have been shown to use nitrate even at low concentrations (Fawcett et al. 2011); nonetheless, the relief of N limitation by addition of excess nitrate could stimulate cells to take up and reduce additional nitrate. Following

**Table 1.** Geometric least squares mean ( $\pm$  1SE) trace metal quotas in pico- and nanoplankton cells ( $\mu\text{mol TM Mol C}^{-1}$ ) from this study and others, measured by SXRF.

Location	Cell type	Mn:C	<i>n</i>	Fe:C	<i>n</i>	Co:C	<i>n</i>	Ni:C	<i>n</i>	Zn:C	<i>n</i>
W. Atlantic	Nano	$2.1 \pm 1^{a,b}$	4	$6.2 \pm 4$	4	$1.2 \pm 0.5^{a,b}$	3	$2.5 \pm 1^{a,b}$	5	$35 \pm 19^b$	5
W. Atlantic	Pico	$3.6 \pm 2$	7	$18 \pm 5$	7	$6.1 \pm 2$	4	$3 \pm 1$	5	$49 \pm 17^b$	7
E. Atlantic	Pico	$2.7 \pm 0.7$	13	$12 \pm 2$	15	$3.0 \pm 0.7$	8	$3.9 \pm 1$	14	$27 \pm 4.9^b$	15
Indian	Nano	$0.7 \pm 0.1^a$	18	$5.0 \pm 1$	18	$0.6 \pm 0.09^a$	18	$0.51 \pm 0.1^a$	17	$6.8 \pm 1.5^a$	17
Indian	Pico	$1.5 \pm 0.3$	16	$8.8 \pm 2$	19	$1.2 \pm 0.3$	16	$1.3 \pm 0.4$	18	$7.6 \pm 2.4^a$	18
Southern	Nano	$3.1 \pm 0.6^b$	20	$6.5 \pm 1$	19	$1.1 \pm 0.2^b$	15	$1.4 \pm 0.4^b$	19	$9.1 \pm 1.4^a$	19
N. Atlantic*		$3.2 \pm 0.4$		$35 \pm 2$		$0.92 \pm 0.11$		$1.6 \pm 0.3$		$25 \pm 3$	
E. Pacific†		$7 \pm 4$	60	$12 \pm 5$	60			$3.3 \pm 0.6$	58	$40 \pm 10$	61
N. Atlantic	<i>Syn</i>	$9 \pm 2$	8	$30 \pm 4$	5			$13 \pm 5$	8	$64 \pm 16$	8

Phytoplankton cell type is abbreviated nano = nanoeukaryotes, pico = picoeukaryotes, *Syn* = *Synechococcus*; *n* refers to number of individual cells. Super-scripted letters indicate significantly different groups (post hoc Tukey HSD) within each size class for this study. Iron quotas were not significantly different across regions within either size class. Mn, Ni and Co picoplankton quotas were not significantly different across regions.

\*Autotrophic flagellates (Twining et al. 2015).

†Offshore > 2 km (Twining et al. 2021).

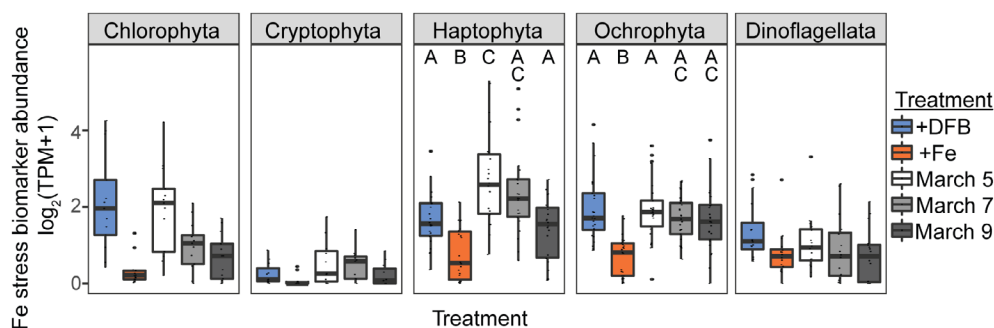


**Fig. 3.** Iron status of Southern Ocean flagellate communities. Comparison of the normalized expression ( $\log_2[\text{TPM} + 1]$ , transcripts-per-million) of the most abundant iron stress genes, Flavodoxin and Fea, for each plankton class across low Fe (added DFB), high Fe (added Fe), and in situ surface samples (15 m). Protein sequences were queried against a database of one Fea and five Flavodoxin PFAMs; hits with an e-value threshold  $< 10^{-10}$  were further filtered to those genes representing  $> 1\%$  of total transcriptome abundance. Significantly different transcript abundances between treatments were found among all taxa except dinoflagellates (Kruskal–Wallis  $p < 0.05$ ), with letters indicating groupings detected by post hoc Dunn's test.

nitrate addition to the high-Fe, oligotrophic W. Atlantic, Fe quotas doubled from  $13 \pm 1$  to  $25 \pm 1 \mu\text{mol Fe mol C}^{-1}$  (Fig. 2B,  $p = 0.01$ ) and bulk Chl *a* concentrations increased (Fig. S2). This region has sufficient dFe available for cells to take up more Fe when needed, and cells may maintain a lower Fe quota when not meeting the demand of high nitrate assimilation. Macronutrients may thus be as important as trace metal availability for controlling the metal contents of small autotrophic flagellates, within the context of low physiological plasticity.

In addition to Fe, we measured other biogenic metals in small flagellates (Table 1). The quotas of other trace elements were more similar than Fe to quotas previously measured in small flagellates in the North Atlantic during a winter study (Twining et al. 2015) and in the equatorial Pacific (Twining et al. 2011; Fig. S4). For all metals, quotas in the

Indian Ocean were in the lowest regional grouping. Quotas of Mn, Zn, and Co varied slightly across regions. Like Fe, quotas of Mn, Ni, and Zn were low and fairly constrained compared to the known ranges of other groups (Twining and Baines 2013). Quotas in a limited number of co-occurring *Synechococcus* that we analyzed were higher than the flagellates (Table 1).

Our samples spanned a range of dZn (Fig. 1), and we also examined relationships of Zn quotas with dZn, region, and macronutrient availability. As for Fe, we saw little evidence for Zn limitation: Chl *a* concentrations increased with N, N + Zn, or N + Fe addition, but not with Zn addition alone (Fig. S2a). Zinc quotas were not directly related to Zn concentration ( $p = 0.34$ ) but were higher at stations with greater Zn availability in Indian Ocean, where dissolved inorganic phosphorus (DIP) concentrations were low (Fig. 1C). In regions of low DIP, plankton access dissolved organic phosphorus using

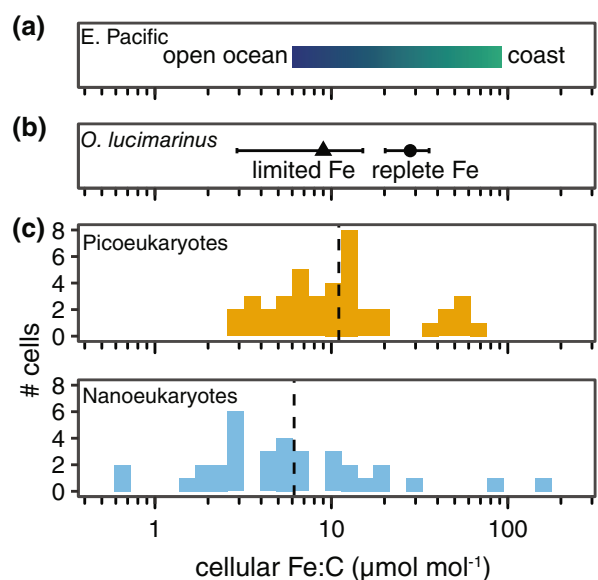


**Fig. 4.** Iron quotas in pico- and nanoeukaryotes. **(A)** Cell quotas of small autotrophic flagellates across a transect from coastal ecosystems to open ocean in the East Pacific (EPZT) as reported by Twining et al. (2021). **(B)** Geometric mean ( $\pm$  SD) cell quotas of *O. lucimarinus* cultured in limited (triangle) and replete (circle) Fe media ( $n = 3$ ). **(C)** Cell quotas of pico- and nanoeukaryotes from four open ocean regions (histograms, geometric means as dashed lines).

alkaline phosphatases (Duhamel et al. 2021), which incorporate Zn, Co, or in the case of bacteria, Fe. Previous studies have shown limited responses of APA to metal addition in communities that are limited by both DIP and the cofactor metal (Mahaffey et al. 2014; Browning et al. 2017). In our work, whole community APA at either terminus of the Fe-dust gradient showed no significant response to Zn or Fe addition (Fig. S2b), and cellular Fe and Zn quotas of small flagellates in these treatments also did not increase above the control (Figs. S6, S2b), consistent both with previous phosphatase studies (Mahaffey et al. 2014; Browning et al. 2017) and with other evidence (Chl *a* and quota responses) that these trace metals were not limiting. Thus, like nitrate, phosphate availability may influence metal quotas along with metal availability.

#### Are picoeukaryotes and nanoeukaryotes functionally distinct?

Biogeochemical models represent many taxa with one pico-/nanophytoplankton functional type. We examined whether pico- and nanoeukaryotes distinguished with a 3  $\mu$ m cut-off (as advocated by Vaulot et al. 2008) had meaningfully different metal contents. Average Fe quotas in picoeukaryotes were twofold higher than those in nanoeukaryotes (Table S3,  $p = 0.007$ ), but the difference between sizes was smaller than the variance observed within each group (Fig. 4C) and smaller than the range of flagellate quotas in previous culture and field studies, e.g., the 40-fold difference in quotas between coastal and open-ocean flagellates (Fig. 4A, Twining

et al. 2021). We found a weak negative relationship between Fe quota and cell volume ( $\log(\text{Fe:C}) = 1.1 - 0.14 \log[\text{volume}]$ ), but cell volume could only explain 4% of the variability in quotas ( $R^2 = 0.04$ ,  $p = 0.03$ ). These trends are also true of three other biologically active trace metals: Mn, Ni, and Co are twice as high in picoeukaryotes as nanoeukaryotes, a difference that is statistically significant ( $p = 0.01$ ,  $0.03$ , and  $0.0003$ , respectively) yet small relative to the variance within each group (Table S3). Zinc quotas were not statistically different between sizes ( $17 \pm 6$  [pico] and  $15 \pm 6$  [nano]  $\mu\text{mol Zn mol C}^{-1}$ ,  $p = 0.6$ ). Considering these size classes as one group for our analysis afforded us greater statistical power than using unbalanced size-segregated data to compare across regions. The metal contents of these size classes are more similar to one another than to other groups, justifying their representation by one functional type while also presenting opportunities for further studies to resolve taxonomic differences.

#### Implications

The relatively narrow ranges of quotas found for small flagellates across a broad range of dFe suggest that physiological and ecological traits of small autotrophic flagellates are distinct from cyanobacteria, diatoms, and even larger flagellated phototrophs. In natural plankton assemblages and in culture, small flagellates operated at the lower range of Fe quotas typically observed for diatoms. This is an important distinction since our current understanding of phytoplankton metal physiology comes mostly from work with diatoms, but smaller taxa also play a key role in the ecology and chemistry of these regions. Remaining questions regarding specific physiological adaptations of different taxa within this diverse group of small flagellates, as well as further field studies of single-cell diazotroph responses to metal availability, will require new methods that can pair biological classification and chemical measurements. These findings can be used to update parameters in biogeochemical models to reflect the distinct physiology of pico-/nanophytoplankton to better constrain predictions of future productivity under changing environmental conditions.

#### References

- Artigue, L., and others. 2020. Water mass analysis along 22 °N in the subtropical North Atlantic for the JC150 cruise (GEOTRACES, GApr08). *Deep Sea Res. Oceanogr. Res. Pap.* **158**: 103230. doi:10.1016/j.dsr.2020.103230
- Aumont, O., C. Ethé, A. Tagliabue, L. Bopp, and M. Gehlen. 2015. PISCES-v2: An ocean biogeochemical model for carbon and ecosystem studies. *Geosci. Model Dev.* **8**: 2465–2513. doi:10.5194/gmd-8-2465-2015
- Behnke, J., and J. LaRoche. 2020. Iron uptake proteins in algae and the role of iron starvation-induced proteins (ISIPs). *Eur. J. Phycol.* **55**: 339–360. doi:10.1080/09670262.2020.1744039
- Botebol, H., and others. 2017. Acclimation of a low iron adapted *Ostreococcus* strain to iron limitation through

- cell biomass lowering. *Sci. Rep.* **7**: 327. doi:[10.1038/s41598-017-00216-6](https://doi.org/10.1038/s41598-017-00216-6)
- Browning, T. J., E. P. Achterberg, J. C. Yong, I. Rapp, C. Utermann, A. Engel, and C. M. Moore. 2017. Iron limitation of microbial phosphorus Acquisition in the Tropical North Atlantic. *Nat. Commun.* **8**: 15465. doi:[10.1038/ncomms15465](https://doi.org/10.1038/ncomms15465)
- Cohen, N. R., and others. 2018. Iron storage capacities and associated ferritin gene expression among marine diatoms. *Limnol. Oceanogr.* **63**: 1677–1691. doi:[10.1002/lno.10800](https://doi.org/10.1002/lno.10800)
- Cuvelier, M. L., and others. 2010. Targeted metagenomics and ecology of globally important uncultured eukaryotic phytoplankton. *Proc. Natl. Acad. Sci. U. S. A.* **107**: 14679–14684. doi:[10.1073/pnas.1001665107](https://doi.org/10.1073/pnas.1001665107)
- Duhamel, S., J. M. Diaz, J. C. Adams, K. Djaoudi, V. Steck, and E. M. Waggoner. 2021. Phosphorus as an integral component of global marine biogeochemistry. *Nat. Geosci.* **14**: 359–368. doi:[10.1038/s41561-021-00755-8](https://doi.org/10.1038/s41561-021-00755-8)
- Erdner, D. L., and D. M. Anderson. 1999. Ferredoxin and flavodoxin as biochemical indicators of iron limitation during open-ocean iron enrichment. *Limnol. Oceanogr.* **44**: 1609–1615. doi:[10.4319/lo.1999.44.7.1609](https://doi.org/10.4319/lo.1999.44.7.1609)
- Fawcett, S. E., M. W. Lomas, J. R. Casey, B. B. Ward, and D. M. Sigman. 2011. Assimilation of upwelled nitrate by small eukaryotes in the Sargasso Sea. *Nat. Geosci.* **4**: 717–722. doi:[10.1038/ngeo1265](https://doi.org/10.1038/ngeo1265)
- Flynn, K. J. 2010. Ecological modelling in a sea of variable stoichiometry: Dysfunctionality and the legacy of Redfield and Monod. *Prog. Oceanogr.* **84**: 52–65. doi:[10.1016/j.pocean.2009.09.006](https://doi.org/10.1016/j.pocean.2009.09.006)
- Gilbert, N. E., and others. 2022. Bioavailable iron titrations reveal oceanic *Synechococcus* ecotypes optimized for different iron availabilities. *ISME Commun.*
- Hirata, T., and others. 2011. Synoptic relationships between surface chlorophyll a and diagnostic pigments specific to phytoplankton functional types. *Biogeosciences* **8**: 311–327. doi:[10.5194/bg-8-311-2011](https://doi.org/10.5194/bg-8-311-2011)
- Kunde, K., N. J. Wyatt, D. González-Santana, A. Tagliabue, C. Mahaffey, and M. C. Lohan. 2019. Iron distribution in the subtropical North Atlantic: The pivotal role of colloidal iron. *Global Biogeochem. Cycles* **33**: 1532–1547. doi:[10.1029/2019GB006326](https://doi.org/10.1029/2019GB006326)
- Mahaffey, C., S. Reynolds, C. E. Davis, and M. C. Lohan. 2014. Alkaline phosphatase activity in the Subtropical Ocean: Insights from nutrient, dust and trace metal addition experiments. *Front. Mar. Sci.* **1**: 73. doi:[10.3389/fmars.2014.00073](https://doi.org/10.3389/fmars.2014.00073)
- Menden-Deuer, S., and E. J. Lessard. 2000. Carbon to volume relationships for dinoflagellates, diatoms, and other Protist plankton. *Limnol. Oceanogr.* **45**: 569–579. doi:[10.4319/lo.2000.45.3.0569](https://doi.org/10.4319/lo.2000.45.3.0569)
- Moore, C. M., and others. 2013. Processes and patterns of oceanic nutrient limitation. *Nat. Geosci.* **6**: 701–710. doi:[10.1038/ngeo1765](https://doi.org/10.1038/ngeo1765)
- Moore, J. K., and others. 2018. Sustained climate warming drives declining marine biological productivity. *Science* **359**: 1139–1143. doi:[10.1126/science.aao6379](https://doi.org/10.1126/science.aao6379)
- Peers, G., and N. M. Price. 2006. Copper-containing plastocyanin used for electron transport by an oceanic diatom. *Nature* **441**: 341–344. doi:[10.1038/nature04630](https://doi.org/10.1038/nature04630)
- Roche, J. L., P. W. Boyd, R. Michael, L. McKay, and R. J. Geider. 1996. Flavodoxin as an in situ marker for iron stress in phytoplankton. *Nature* **382**: 802–805. doi:[10.1038/382802a0](https://doi.org/10.1038/382802a0)
- Rusch, D. B., A. C. Martiny, C. L. Dupont, A. L. Halpern, and J. Craig Venter. 2010. Characterization of *Prochlorococcus* clades from iron-depleted oceanic regions. *Proc. Natl. Acad. Sci. U. S. A.* **107**: 16184–16189. doi:[10.1073/pnas.1009513107](https://doi.org/10.1073/pnas.1009513107)
- Schoffman, H., H. Lis, Y. Shaked, and N. Keren. 2016. Iron–nutrient interactions within phytoplankton. *Front. Plant Sci.* **7**: 1223. doi:[10.3389/fpls.2016.01223](https://doi.org/10.3389/fpls.2016.01223)
- Scott, F. J., and H. J. Marchan [eds.]. 2005. *Antarctic marine protists*. Australian Biological Resources Study/Australian Antarctic Division.
- Shire, D. M., and A. B. Kustka. 2015. Luxury uptake, iron storage and ferritin abundance in *Prochlorococcus marinus* (*Synechococcales*) strain MED4. *Phycologia* **54**: 398–406. doi:[10.2216/14-109.1](https://doi.org/10.2216/14-109.1)
- Sofen, L. E., and B. S. Twining. 2021. Trace metal contents of autotrophic flagellates from contrasting open-ocean ecosystems. doi:[10.5281/ZENODO.5191479](https://doi.org/10.5281/ZENODO.5191479)
- Stock, C. A., J. P. Dunne, and J. G. John. 2014. Global-scale carbon and energy flows through the marine planktonic food web: An analysis with a coupled physical–biological model. *Prog. Oceanogr.* **120**: 1–28. doi:[10.1016/j.pocean.2013.07.001](https://doi.org/10.1016/j.pocean.2013.07.001)
- Strzepek, R. F., M. T. Maldonado, K. A. Hunter, R. D. Frew, and P. W. Boyd. 2011. Adaptive strategies by Southern Ocean phytoplankton to lessen iron limitation: Uptake of organically complexed iron and reduced cellular iron requirements. *Limnol. Oceanogr.* **56**: 1983–2002. doi:[10.4319/lo.2011.56.6.1983](https://doi.org/10.4319/lo.2011.56.6.1983)
- Sunda, W. G., and S. A. Huntsman. 1995. Iron uptake and growth limitation in oceanic and coastal phytoplankton. *Mar. Chem.* **50**: 189–206. doi:[10.1016/0304-4203\(95\)00035-P](https://doi.org/10.1016/0304-4203(95)00035-P)
- Tagliabue, A., and others. 2020. An iron cycle Cascade governs the response of equatorial Pacific ecosystems to climate change. *Glob. Chang. Biol.* **26**: 6168–6179. doi:[10.1111/gcb.15316](https://doi.org/10.1111/gcb.15316)
- Tomas, C. R. [ed.]. 1997. *Identifying marine phytoplankton*. Elsevier. doi:[10.1016/B978-0-12-693018-4.X5000-9](https://doi.org/10.1016/B978-0-12-693018-4.X5000-9)
- Twining, B. S., S. B. Baines, J. B. Bozard, S. Vogt, E. A. Walker, and D. M. Nelson. 2011. Metal quotas of plankton in the equatorial Pacific Ocean. *Deep-Sea Res. Top. Stud. Oceanogr.* **58**: 325–341. doi:[10.1016/j.dsr2.2010.08.018](https://doi.org/10.1016/j.dsr2.2010.08.018)
- Twining, B. S., and S. B. Baines. 2013. The trace metal composition of marine phytoplankton. *Ann. Rev. Mar. Sci.* **5**: 191–215. doi:[10.1146/annurev-marine-121211-172322](https://doi.org/10.1146/annurev-marine-121211-172322)
- Twining, B. S., S. Rauschenberg, P. L. Morton, and S. Vogt. 2015. Metal contents of phytoplankton and labile



- particulate material in the North Atlantic Ocean. *Prog. Oceanogr.* **137**: 261–283. doi:[10.1016/j.pocean.2015.07.001](https://doi.org/10.1016/j.pocean.2015.07.001)
- Twining, B. S., S. Rauschenberg, S. E. Baer, M. W. Lomas, A. C. Martiny, and O. Antipova. 2019. A nutrient limitation mosaic in the eastern tropical Indian Ocean. *Deep Sea Res. Top. Stud. Oceanogr.* **166**: 125–140. doi:[10.1016/j.dsr2.2019.05.001](https://doi.org/10.1016/j.dsr2.2019.05.001)
- Twining, B. S., and others. 2021. Taxonomic and nutrient controls on phytoplankton iron quotas in the ocean. *Limnol. Oceanogr. Lett.* **6**: 96–106. doi:[10.1002/lol2.10179](https://doi.org/10.1002/lol2.10179)
- Vaulot, D., W. Eikrem, M. Viprey, and H. Moreau. 2008. The diversity of small eukaryotic phytoplankton ( $\leq 3$   $\mu$ m) in marine ecosystems. *FEMS Microbiol. Rev.* **32**: 795–820. doi:[10.1111/j.1574-6976.2008.00121.x](https://doi.org/10.1111/j.1574-6976.2008.00121.x)
- Wang, S., S. Elliott, M. Maltrud, and P. Cameron-Smith. 2015. Influence of explicit *Phaeocystis* parameterizations on the global distribution of marine dimethyl sulfide. *J. Geophys. Res. Biogeo.* **120**: 2158–2177. doi:[10.1002/2015JG003017](https://doi.org/10.1002/2015JG003017)
- Zhang, H.-R., Y. Wang, P. Xiu, Y. Qi, and F. Chai. 2021. Roles of iron limitation in phytoplankton dynamics in the Western and eastern subarctic Pacific. *Front. Mar. Sci.* **8**: 735826. doi:[10.3389/fmars.2021.735826](https://doi.org/10.3389/fmars.2021.735826)
- experiments in the Atlantic and for measuring dFe, dZn, and APA, respectively. We thank Philip Boyd for assistance with work at the Southern Ocean Time Series and helpful comments on the manuscript. Use of the Advanced Photon Source, an Office of Science User Facility operated for the U.S. Department of Energy (DOE) Office of Science by Argonne National Laboratory, was supported by the U.S. DOE under Contract No. DE-AC02-06CH11357. Transcriptomic sequencing (proposal ID 504140) conducted by the U.S. Department of Energy Joint Genome Institute (<https://ror.org/04xm1d337>), a DOE Office of Science User Facility, is supported by the Office of Science of the U.S. Department of Energy under Contract No. DE-AC02-05CH11231. L.E.S. and B.S.T. were supported by NSF grants OCE-1829819 and OCE-1559021. N.E.G. and S.W.W. were supported by NSF grant OCE-1829641. M.C.L. was supported by UK Natural Environment Research Council grant NE/N001125/1. C.M. was supported by UK Natural Environment Research Council grant NE/N001079/1. This research was financially supported under Australian Research Council's Discovery program (DP170102108; DP130100679) and ship time from Australia's Marine National Facility. We are grateful to the officers, crew, and research staff of the Marine National Facility and the *R.V. Investigator* for their help with sample collection and generation of hydrochemistry data. We thank two anonymous reviewers for thoughtful comments on this manuscript.

Submitted 22 October 2021

Revised 22 March 2022

Accepted 27 April 2022

#### Acknowledgments

We thank Sara Rauschenberg for assisting with SXRF analyses. We thank Koko Kunde, Neil Wyatt, and Clare Davies for assisting in the incubation